

Experimental and numerical characterization of floc morphology: role of changing hydraulic retention time under flocculation mechanisms

Jun Nan¹ · Meng Yao¹ · Ting Chen¹ · Zhenbei Wang¹ · Qinggui Li¹ · Dan Zhan¹

Received: 16 June 2015 / Accepted: 5 October 2015 / Published online: 21 October 2015
© Springer-Verlag Berlin Heidelberg 2015

Abstract The formation, breakage, and re-growth of flocs were investigated by using modified flocculation tests and numerical simulation to explore the evolution of floc morphology for different hydraulic retention times. The shorter the aggregation time was, the smaller the flocs produced for the same hydraulic conditions were. Another interesting discovery was that broken flocs that formed in shorter aggregation time had the capacity to completely recover, whereas those formed in a longer amount of time had rather worse reversibility of broken flocs. With the addition of the maximum motion step in the representative two-dimensional diffusion-limited aggregation (DLA) model, there was a transition for flocs from isotropic to anisotropic as the maximum motion step increased. The strength of flocs was mainly affected by the distribution of particles near the aggregated core rather than distant particles. A simplified breakage model, which found that broken flocs provided more chances for diffused particles to access the inner parts of flocs and to be uniformly packed around the aggregated core, was first proposed. Moreover, an important result showed that the floc fragments formed with a larger value of the maximum motion step had more growing sites than did those with a smaller m_{sa} value, which was a benefit of following the re-forming procedure.

Keywords Floc breakage · Floc re-growth · Hydraulic retention time · DLA model

Introduction

Coagulation and flocculation are widely used in the solid/liquid separation process and are normally used for the removal of turbidity and natural organic matter (NOM) (Wenzheng 2010; Yukselen and Gregory 2004). Flocs formed in the water treatment process are considered a type of colloidal substance. The structure of large flocs changes continually due to the breakup of the flocs' internal bonds and re-forming at more favorable points during the aggregation process (Biggs and Lant 2000). Typical drinking water treatments are always designed to weaken the effect of floc breakage; nevertheless, in reality, this often is not the case, with regions of high shear being popular (McCurdy et al. 2004). Although the major coagulation mechanisms and the optimization of operational parameters have been studied for many years, knowledge of the floc growth mechanism remains limited (Zhong et al. 2011). Therefore, the evolution of floc morphological characterization should be considered for overall process optimization and has been the subject of in-depth research in recent years (Dong et al.; Turchiuli and Fargues 2004; Wang et al. 2011; Yu et al. 2012).

A number of lectures have reported that the dosage and species of a reagent, especially the dosage strategy, have an important influence on the different recovery degrees of broken flocs (Wei et al. 2009; Xu et al. 2010). However, hydraulic retention time (HRT) has received relatively little attention. Wahlberg et al. (1994) showed that activated sludge flocculated by mechanical means grew rapidly by 99 % within 10 min under batch conditions. Under the same conditions, the properties and configuration of flocs formed during the whole

Responsible editor: Marcus Schulz

✉ Jun Nan
nanjun_219@163.com

¹ Skate Key Laboratory of Urban Water Resource and Environment, School of Municipal and Environmental Engineering, Harbin Institute of Technology, Harbin 150090, People's Republic of China

flocculation process could change intensively for different reaction times because flocculation treatment does not always run on a rated flow in a real process. Therefore, it is essential to pay a great deal of attention to understanding the behavior of flocs for different reaction times.

A groundbreaking fractal growth model named diffusion-limited aggregation (DLA) was originally proposed to describe the aggregate procedure of inorganic particles, such as ferric, zinc, and silicon dioxide (Witten and Sander 1981). Despite its simple growing rules, the DLA model can still display a much more real and fractal phenomenon, which provides detailed information to further investigate the structure of agglomerates (Parkinson et al. 1999). Recently, research on the DLA model has become popular, but most of these studies focused on the physical growth mechanism and properties of aggregation (Higashitani et al. 2001; Nan et al. 2009; Yao et al. 2014; Zhao et al. 2011). There seemed to be a lack of combination between the theoretical model and practical application. Several lectures have stated that suspended particles move in the orthokinetic regime under shear force, which means that all particles move in the same direction (Hopkins and Ducoste 2003; Mpofu et al. 2003). To study the growing approach of a single floc during flocculation treatment, a hypothesis was proposed in which the random motion of a particle was the main reason for formation of the fractal structure of a floc on the condition that the same direction rotation of each particle is ignored. Based on this hypothesis, the two-dimensional DLA model can be used to investigate the single floc growth procedure under a shear flow field.

This work aimed to investigate the impact of different HRT on clay-polyaluminum chloride (PACl) flocs and develop a better understanding of the mechanism underlying the aggregation, breakage, and re-growth processes. A series of modified flocculation tests were conducted under different aggregation and re-growth time. Aggregation time has an impact on the size distribution of broken flocs, and the reversibility of broken flocs decreased as condensation time increased. Moreover, the second breakage of re-grown flocs most likely occurred at longer re-growing time, which was possibly attributed to the strength of flocs decreasing as reaction time became too long. For the sake of deeply figuring out the changes of floc properties for different times, an improved two-dimensional DLA model with the addition of maximum motion steps was used to simulate the growing process of flocs, which allowed a study of the dynamic variation of floc nature in the static model. Then, the formed virtual floc was ruptured using a breakage method, which was first proposed to imitate the actual breaking process. The re-growing stage also proceeded based on these broken virtual flocs. Through the statistics of virtual floc characteristic parameters, there was a transition of virtual flocs from anisotropic to isotropic after breakage, and broken flocs provided many more adhesion sites around the aggregated cores to which scattered particles

could stick, which optimized the properties of re-grown flocs. The improved understanding of this process should be a significant addition of knowledge to the field of particle coagulation and removal.

Materials and methods

Stock solution and coagulant

Kalolin clay (Taijin, China) was dissolved in the tap water of Harbin, China, with a similar preparation to that of Yukelen and Gregory (Yukselen and Gregory 2004). The final clay concentration was 100 mg/L. Harbin tap water has medium total hardness (ca. 160 mg/L as CaCO_3) and alkalinity (ca. 115 mg/L as CaCO_3) and a pH of approximately 7.8. To avoid the disturbance of divalent metal ions such as Ca^{2+} and Mg^{2+} in tap water, a small dosage of humic acid (Shanghai, China) was added to the stock solution. The final suspension contained 100 mg/L kaolin and 2 mg/L humic acid and had a turbidity of approximately 100 NTU, as determined by an online turbidimeter (700AQ, WTW, Germany). The particles in the testing water had an average size of approximately 3 μm , as measured by using an online particle counter (2200PCX, HACH, USA).

PACl was used as the coagulant. Stock PACl solutions of 1 % w/w were prepared at a concentration of 0.1 M in deionized (DI) water (5 g dissolved in deionized water to 500 mL). This solution was used directly, i.e., without prior preparation.

Apparatus

A modified cubic reactor was applied in these flocculation tests and had a bottom length $D=150$ mm and a liquid height $H=150$ mm; it was filled with 3.4 L of testing water sample as the working fluid. A R1342-type impeller (IKA, Germany) with a diameter $d=50$ mm was used for agitation, and the center of the impeller was placed at $C=H/3$ from the tank bottom. This N-type multiple velocity agitator, named Euro Star, could realize online monitoring and has been successively used in some of our previous studies (Yao et al. 2014, 2015, 2016).

From the moment of coagulant addition, a non-intrusive optical sampling method was used to capture images of the particles throughout the flocculation process, including aggregation, breakage, and re-growth. The size and structural properties of the developed flocs were analyzed by using these digital pictures, especially when calculating the fractal dimension. The lack of sample handling throughout the procedure meant that there was nothing to be afraid of regarding the disturbance characteristics of flocs during the measurements and that the accuracy of results could be ensured (Chakraborti et al. 2000). The in situ recognition system consisted of an

Fig. 1 Flowchart of experimental equipment

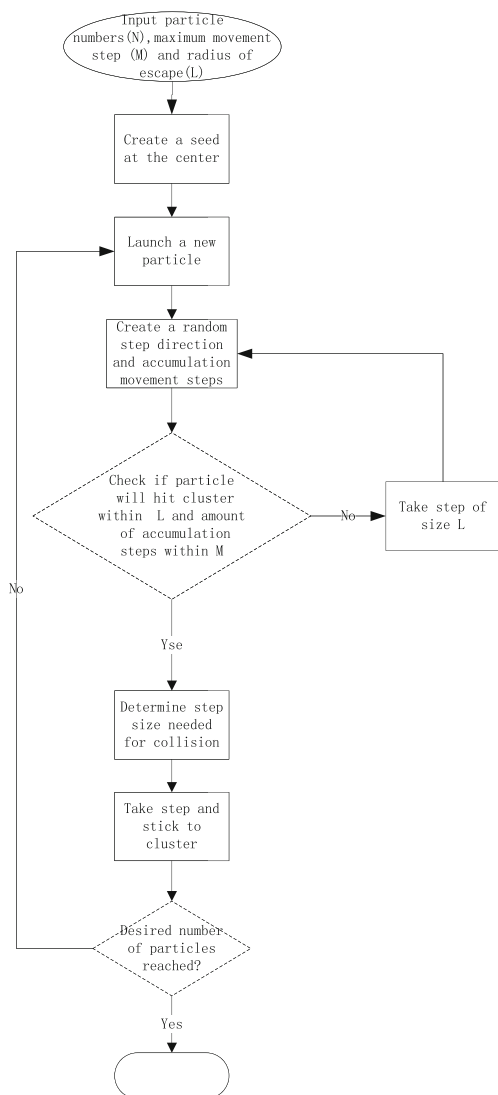
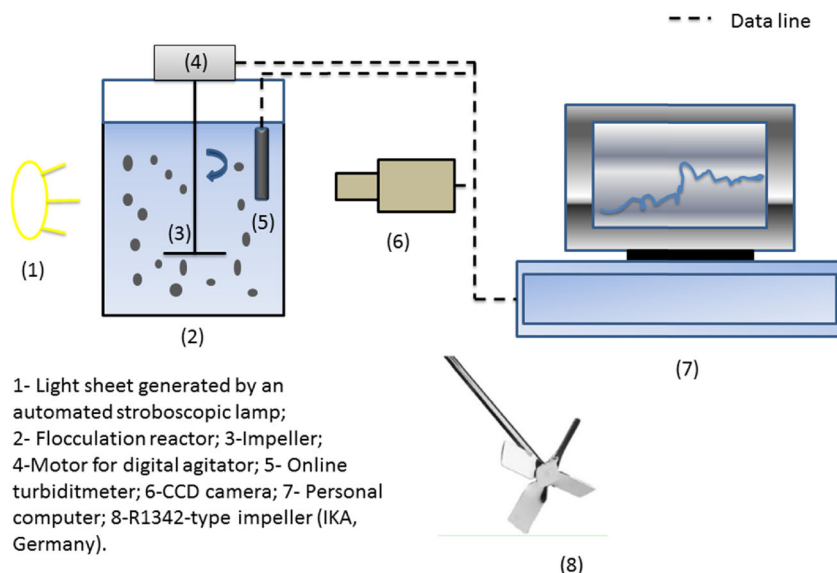


Fig. 2 Flowchart of the off-lattice DLA algorithm

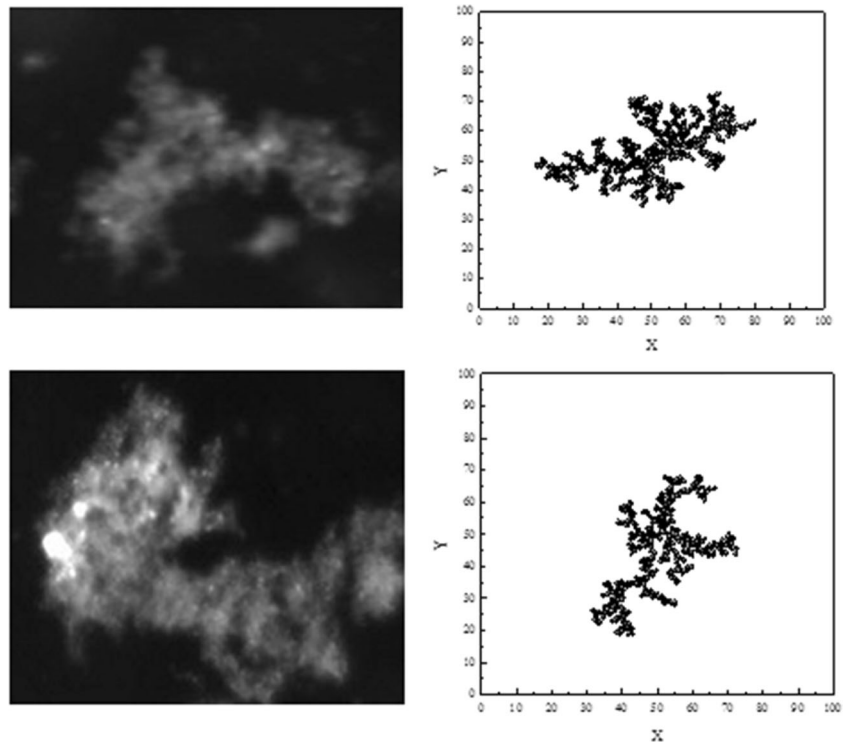
automated stroboscopic lamp, which was used to illuminate suspended particles in the reactor, and a high-speed digital charged-coupled device (CCD) video camera (GmbH, Germany) with a resolution of 992 (horizontal) × 510 (vertical) pixels, which was used to capture particles. The interrogation window was approximately 5665 × 2920 μm. The monitoring system thus had a resolution of approximately 5.7 mm for particle imaging in the present flocculation study. The process control and image processing software package (FMans 10, China) was used to determine the geometrical parameters of the flocs. This device is an independent research achievement of our team and has also been extensively used in our previous studies (He et al. 2012; Nan and He 2012); the detailed configuration is shown in Fig. 1. Based on the real-time and online monitoring of agglomerate geometry and size distribution, the temporal evolution of floc characteristics could be easily studied.

Procedure

The stock solution was diluted in the tap water to 3.4 L and was rapidly mixed at 400 rpm/min until turbidity of the water stability. The optimal PACl dosage was first determined by performing a series of flocculation tests with different coagulant doses (between 1 and 10 mg/L as Al). The stirring speed was set at 400 rpm/min for 30 s and 100 rpm/min for 20 min. Then, the turbidity of the supernatant (at 5 cm below the liquid surface) was measured after 20 min of sedimentation. The amount of coagulant giving the minimum turbidity was the optimal dosage used for all other tests in this study (Duan and Gregory 1998).

PACl solution was added after allowing for 1 min of steady-state turbidity, and the suspension was rapidly mixed at 400 rpm/min ($G \approx 175 \text{ s}^{-1}$) for 30 s to destabilize the

Fig. 3 Comparison between real and virtual flocs



particles. To investigate the evolution of floc morphology with different HRT, two modes of flocculation processes were used. The first one included slow stirring speed of 94 rpm/min ($G \approx 20 \text{ s}^{-1}$) for 10, 15, 20, and 25 min, respectively. After stirring at 300 rpm/min ($G \approx 1413 \text{ s}^{-1}$) for 1 min to cause breaking, the stirring speed was reduced to 94 rpm/min for 15 min to allow the flocs to re-grow. In the second mode of this process, the slow stirring speed of 94 rpm/min was used for 20 min and 300 rpm/min was used for 1 min to break the flocs; then, the speed was reduced to 94 rpm/min for 5, 10, 15, and 20 min to recover the flocs. During these methods, the average size and fractal dimension of each floc was measured by the online monitoring devices.

Fractal dimension of floc by image analysis

The size, d_p , of a floc of irregular shape can be calculated in terms of the equivalent diameter using

$$d_p = (4A/\pi)^{1/2} \tag{1}$$

where A is the projected area of the floc. Then, the average size and size distribution of flocs in more than ten images for a minute were used to reflect the floc size at the corresponding moment. In fractal theory, fractal refers to the formation of a part that bears a certain resemblance to the whole body, emphasizing the formed object with self-similarity and scale

Fig. 4 Schematic of radius of gyration (a) and characteristic length (b) for two-dimensional DLA virtual floc

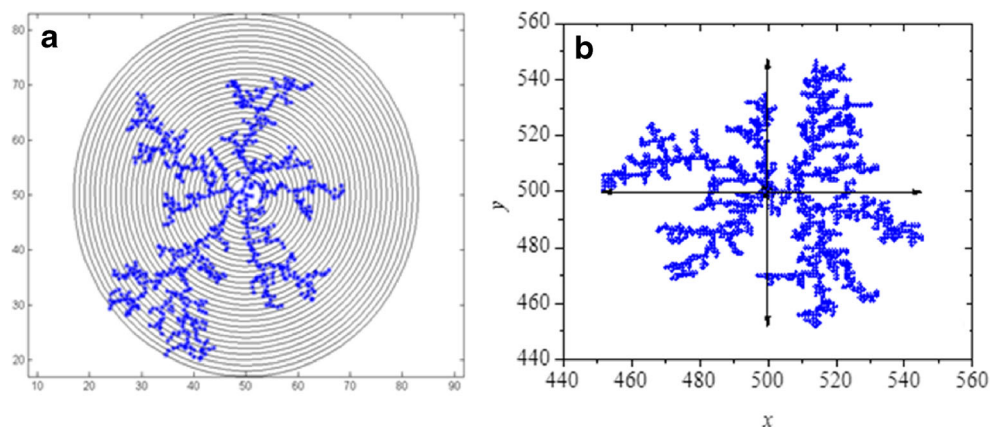
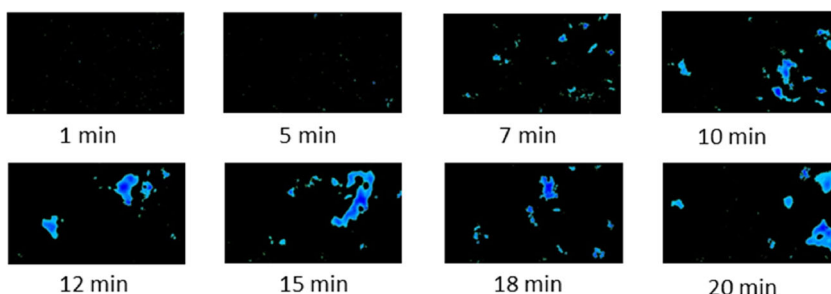


Fig. 5 Variation of floc morphology in the flocculation experiment



invariance (Xiao et al. 2011). To accurately describe the dynamic process of floc growth, a boundary fractal dimension was applied to characterize the fractal properties of flocs. For a two-dimensional projected particle image, the projected area of the particles, which scales up with the length of the perimeter, was defined as the boundary fractal dimension (D_{pf}) (Meakin and Vicsek 1987), which was calculated according to

$$A \propto P^{2/D_{pf}} \tag{2}$$

where P is the perimeter of an aggregate and D_{pf} is based on the perimeter-based fractal dimension of the floc. This D_{pf} ranges from 1 (for the projected area of a sphere) to 2 (for a line) (He et al. 2012). Some lectures have reported that typical values of D_{pf} at the steady state for aggregates are in the range of 1.1–1.4 (McFarlane et al. 2006; Mpofu et al. 2004; Xiao

et al. 2011). The mass fractal dimension is also a measure of floc structure and varies from 1 (for a line) to 3 (for a sphere). However, there is no direct relation between D_{pf} and the mass fractal dimension. The value of D_{pf} not only essentially reflects the configuration of the projected flocs' images, but it could also reflect the fractal characteristics of particles throughout the flocculation process and provide a new way to study the dynamic variation of flocs.

Growth and breakage mechanisms of two-dimensional DLA model

Aggregated model

Off-lattice simulations of the two-dimensional irreversible aggregation processes were performed using MATrix LABoratory. The flowchart of the off-lattice DLA algorithm is shown in Fig. 2. The original DLA algorithm is carried out by placing a seed particle at the center of a cubic box. Then, far from the seed, a new monomeric particle is released, which wanders stochastically over the lattice at a fixed step length in each direction until it runs into and sticks to the seed particle. If, in the course of the walk, a particle crosses the lattice boundary, it is removed from the model. Then, a new particle is generated, and this process repeats. The successive agglomeration of particles develops a DLA cluster. One method can easily speed up the simulations by enlarging the step sizes or allowing for returning instead of escaping (Amitrano et al. 1991; Meakin and Skjeltorp 1993). Figure 3 shows the comparison with real and virtual flocs. The two pictures of flocs on the left were captured using the high pixel digital camera during a real flocculation process, with D_{pf} values of 1.326 and 1.435, respectively. The virtual flocs formed according to the DLA model mentioned above were placed on the right column, with D_{pf} values of 1.305 and 1.418, respectively. Even the configurations of virtual flocs were less complicated than those of real flocs, and their D_{pf} values were approximate. The results indicated that both of those developed via diffusion

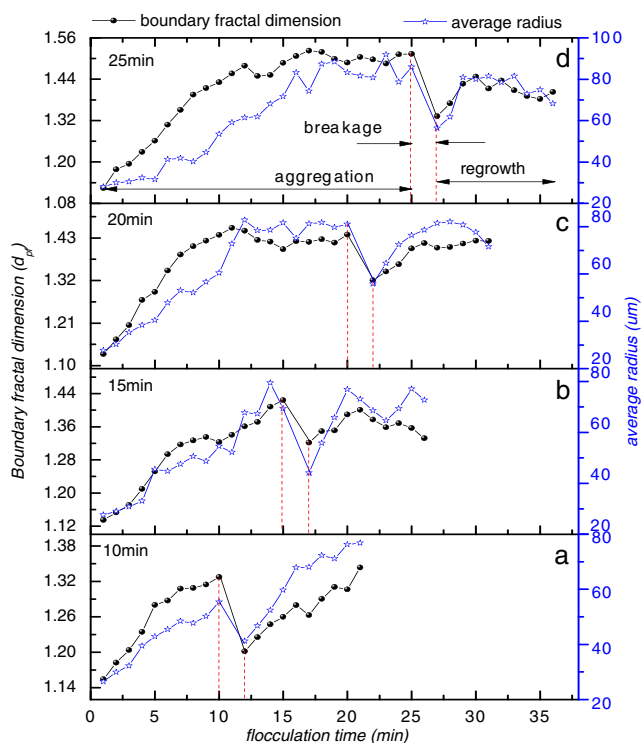


Fig. 6 Variation in average size and boundary fractal dimension during breakage/re-formation under different flocculation times

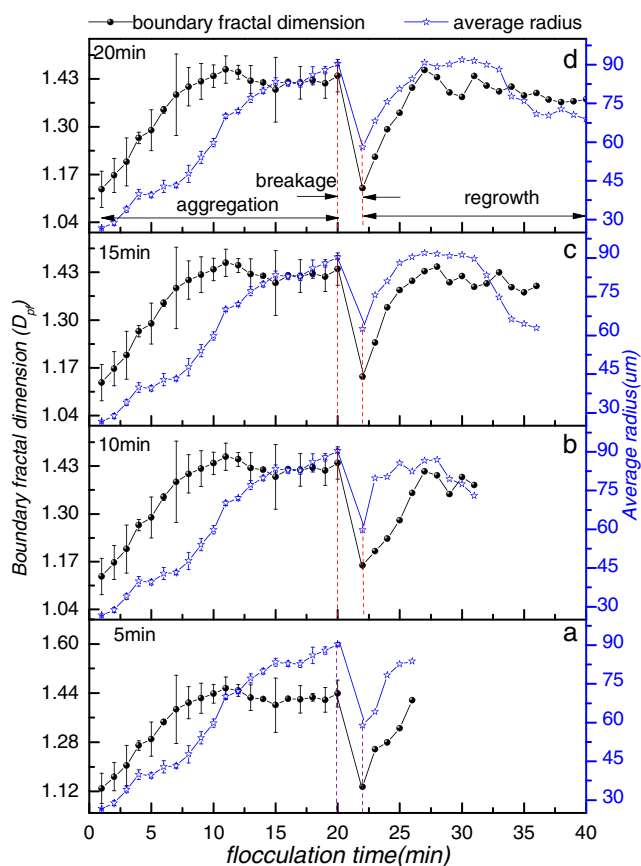
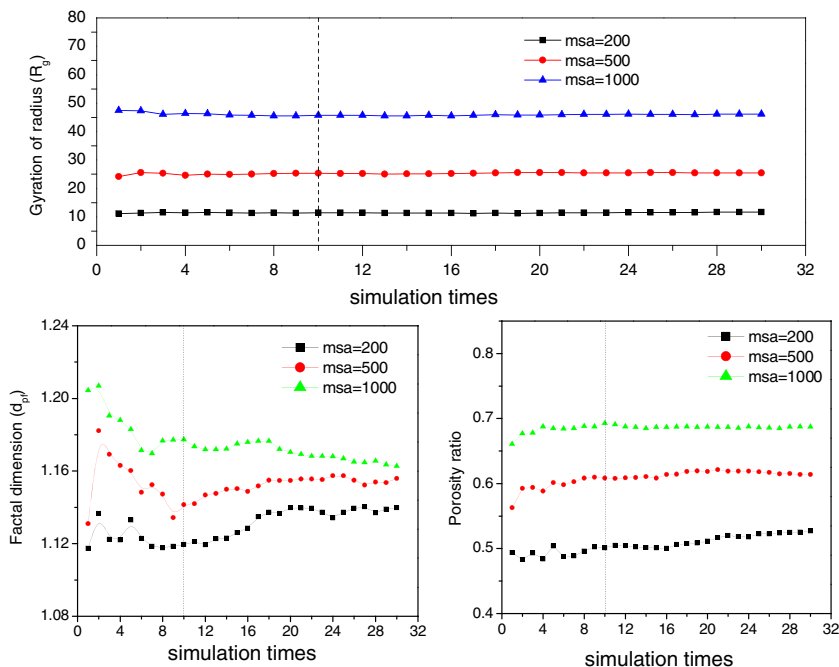


Fig. 7 Variation in average size and boundary fractal dimension during breakage/re-formation under different re-forming times

movement had fractal features because the structures of virtual flocs could represent those of actual flocs.

Fig. 8 Optimization of simulation times under different maximum steps of aggregated particles, *msa*



To investigate the effect of time on the performance of a virtual floc, a pre-set parameter, *M*, was brought into the two-dimensional DLA model to represent the total movement step of a free particle from emergency to adhesion or escape/death. The maximum motion step (*ms*) of a monomeric particle was first introduced in this model and was used to limit the moving time of a free particle. If the value of *M* exceeded the pre-set *ms* value, the free particle was considered to have been removed or escaped from the cubic system. The introduction of *ms* in the numerical simulation process is the equivalent of HRT in the feasible tests, which allow for realizing the dynamic investigation of floc morphology characteristics in the simulation method. For convenience, we defined the maximum motion step in the aggregation stage and that of the regrowth stage as *msa* and *msr*, respectively. By adjusting the value of *ms* in the improved DLA model, the effect of aggregation and re-growth time on the properties of virtual flocs could be investigated efficiently.

Simple breakage model

Surface erosion and large-scale fragmentation are considered two classic modes of floc rupture and have been generally accepted (Jarvis et al. 2005; Mikkelsen and Keiding 2002; Wahlberg et al. 1994; Yeung and Pelton 1996). The surface erosion procedure involves the erosion of small aggregates or primary particles off the parent floc, whereas large-scale fragmentation involves flocs splitting into pieces of a similar size. In this research, a simplified method of floc breakage, referred to as Rumpf

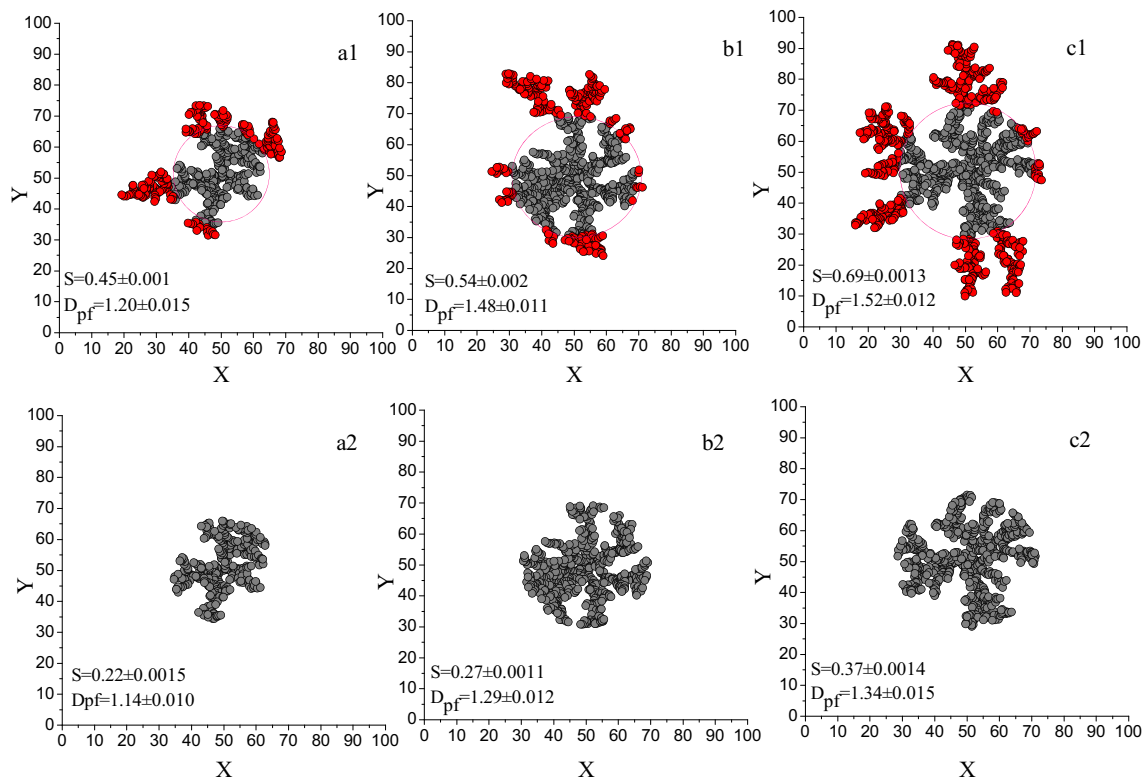


Fig. 9 Morphological characteristics of original and broken virtual flocs under different msa. The notations on the left bottom of every sub-image are porous ratio and fractal dimension of every virtual floc: **a1** aggregated virtual floc on msa=200, **a2** broken virtual floc on msa=200, **b1**

aggregated virtual floc on msa=500, **b2** broken virtual floc on msa=500, **c1** aggregated virtual floc msa=1000, and **c2** broken virtual floc on msa=1000

and Kendall (Rumpf 1962; Kendall et al. 1986), was carried out based on the two classic strength models of flocs; it attained the visualization simulation of the floc aggregation, breakage, and re-growth processes.

The gyration radius of a virtual floc was calculated as follows (Serra et al. 1997):

$$R_g = \left[\sum_{i=1}^N r_i^2 \right]^{1/2} = \left[\frac{1}{N} \sum_{i=1}^N \left((x_i - x_0)^2 + (y_i - y_0)^2 \right) \right]^{1/2}$$

where R_g is the gyration radius of a virtual floc and r_i is the distance between the number i particle (x_i, y_i) and the centroid of the virtual floc (x_0, y_0) .

The coordinates of the centroid were calculated according to Eq. (4):

$$\begin{aligned} x_0 &= \frac{1}{N} \sum_{i=1}^N x_i \\ y_0 &= \frac{1}{N} \sum_{i=1}^N y_i \end{aligned} \tag{4}$$

x_i and y_i are the abscissa and ordinate of the number i particle, respectively.

For the fractal feature of a virtual floc, the boundary fractal dimension mentioned above was also used. The porosity ratio of virtual flocs is the proportion of the number of particles in

Table 1 Each direction characteristic lengths of virtual flocs

Characteristic length	a1	a2	a3	a4	b1	b2	b3	b4	c1	c2	c3	c4
Positive direction of x	18.71	12.79	21.02	23.41	25.39	19.34	25.91	25.29	33.97	21.35	26.71	30.12
Positive direction of y	23.40	15.94	22.65	23.11	26.01	19.26	25.06	28.04	40.03	21.03	23.01	28.92
Negative direction of x	30.70	15.36	19.03	25.21	21.16	19.17	27.58	29.21	23.64	21.115	29.40	31.40
Negative direction of y	18.54	15.64	23.08	27.86	32.89	19.10	23.41	27.63	41.24	21.44	24.37	32.83

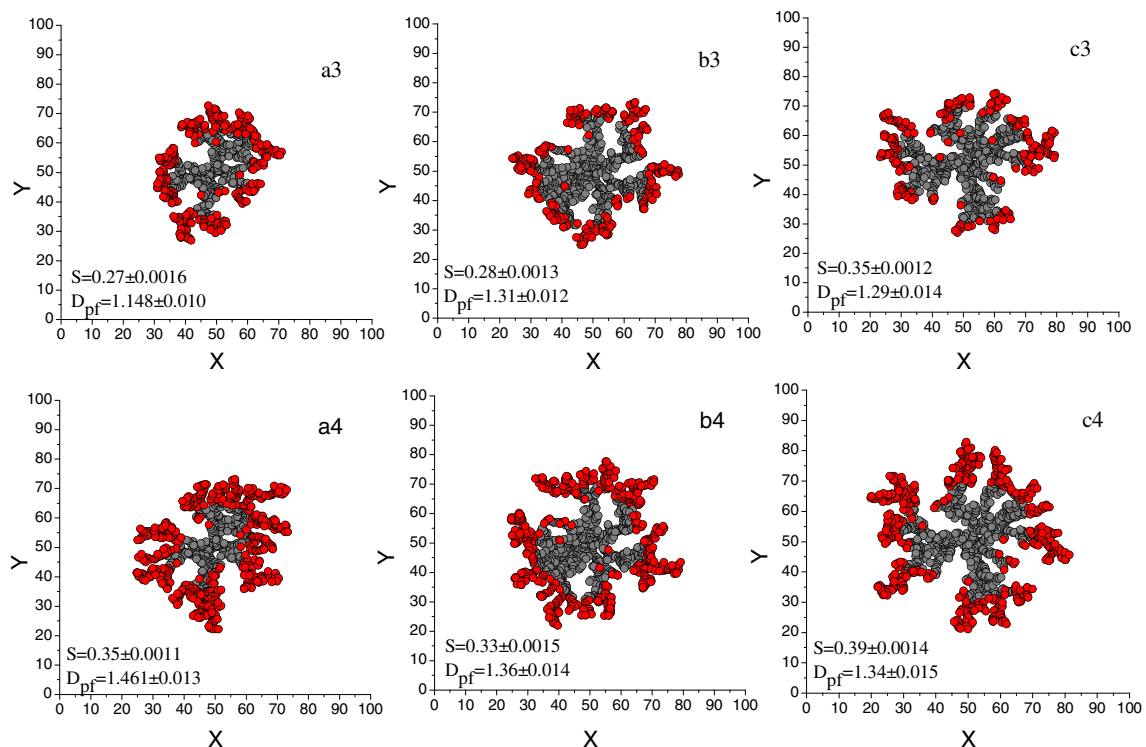


Fig. 10 Morphological characteristics of re-grown virtual flocs under different msr. The notations on the left bottom of every sub-image are porous ratio, and fractal dimensions of every virtual floc **a3** and **a4** are re-grown virtual flocs on msr of 200 and 1000, respectively, under broken

virtual floc formed on msa of 200; **b3** and **b4** are re-grown virtual flocs on msr of 200 and 1000, respectively, under broken virtual floc formed on msa of 500; **c3** and **c4** are re-grown virtual flocs on msr of 200 and 1000, respectively, under broken virtual floc form on msa of 1000

the formed aggregation to the number of grids in the region of the gyration radius. According to this, the porosity ration, *S*, can be expressed as

$$S = 1 - \pi * r^2 N(R_g) / R_g^2 \tag{5}$$

where *r* is the particle radius, pre-set at 0.5, and *N*(*R_g*) is the particle number in the gyration radius.

An example of calculation of the gyration radius is shown in Fig. 4a. A total of 3000 particles were used as the initial condition to start the aggregated process under the pre-set conditions. If the seed seemed to be at the circle center, there was always a maximum gyration radius of the floc. A specific circle with half of the maximum gyration radius was used to cut the original virtual floc, and the remaining part of the floc, located in the inner annulus, was considered the broken virtual floc. Then, considering the broken virtual floc as the core of re-growth, 3000 particles were released successively again into the cubic system and moved according to the DLA model under different msr values to produce new-grown flocs, which simulated the re-growth process. The characteristic parameters of the virtual flocs formed in the aggregation, breakage, and re-growth processes are discussed later.

To describe the anisotropy of virtual flocs, the characteristic lengths of flocs in every direction were applied in the two-

dimensional DLA model. The seed of virtual flocs was set as the central point such that a horizontal and a vertical line pass through this central point. The projection lines of virtual flocs in the *x*-axis and *y*-axis were defined as the characteristic lengths and used to describe the growth of virtual flocs in all directions. A schematic diagram of characteristic lengths is shown in Fig. 4b.

Results and discussion

Characteristic analysis of evolution of floc configuration during flocculation, breakage, and re-growth

Some previous studies have proven that loose and fragile flocs could be broken into smaller pieces but that a significant reversibility of broken clusters is better able to re-form compact and large flocs under appropriate hydraulic conditions (Barbot et al. 2010; Sun et al. 2011; Xu et al. 2010). In this study, a series of modified flocculation tests were carried out on the in situ online monitoring testing platform to investigate the evolution of floc morphological characteristics for various flocculation times. Figure 5 illustrates the variation of floc morphology over the process of flocculation. The initial unstable

particles collided into each other and gathered to gradually grow up. At 15 min, the biggest floc was formed with a fragile and loose structure. As flocs became larger, further growth was restricted by the applied shear for disruptive forces and the collision efficiency of particles in the shear field became lower as particle size increased. Consequently, it could be inferred that flocs experienced a breakage procedure. Broken floc pieces were exhibited at 18 min and then rapidly re-formed via the gentle stirring condition. Comparing the characterizations of flocs formed before and after breakage (at 15 and 20 min in Fig. 5), more compact flocs existed for the latter, which indicated that the structures of broken flocs could be improved during the re-forming stage. The aggregation, breakage, and re-growth of flocs were alternating, repeated processes, and Fig. 5 shows only part of this procedure. Even so, the structures of flocs still differed at every time. Thus, it was necessary to investigate the changes of floc properties over time.

Effect of flocculation time on the evolution of floc structure

The flocculation process is expected to have a major effect on the size and shape of broken and re-grown flocs, which is clearly apparent from the results shown in Fig. 6. With a flocculation time of 10 min, the average radius increased by 27.23 μm and D_{pf} grew from 1.15 to 1.32. A similar growing tendency was found for a flocculation time of 15 min. The larger values of average size and D_{pf} indicated that a higher development degree of flocs began as the reaction time increased. After coagulation for 20 and 25 min, the two monitoring indexes still continuously increased. However, both reached the maximum values nearly simultaneously and then slightly fluctuated near the plateaus. It can be seen that there must be a sufficient amount of time for suspended particles to aggregate into clusters, but the sizes of flocs are not persistent as time increases. Some researchers have stated that flocs would become weaker and even break under the mechanical stirring process (Yukselen and Gregory 2004). Therefore, reasonable coagulation time has an important effect on floc structure and likely plays an equally important role for both broken and re-grown flocs. However, the morphological changes of floc characteristics with reaction time were not easily obtained by using the experimental methods.

It is clear from Fig. 6a, b, c that there were considerable drops in the average radius and fractal dimension immediately after the stirring speed increased to 300 rpm/min. Moreover, the values of both parameters began to increase again after the stirring speed was restored to 94 rpm/min for 15 min, and the different degrees of reversibility of floc breakage occurred during the re-growth stage. It was evident that the broken flocs formed after 10 and 15 min exhibited complete reversibility, as shown in Fig. 6, in which the values of average radius and D_{pf} were always greater than those before breakage. However,

for 20 and 25 min, the average size of flocs displayed limited resilience after the re-growth procedure. The results suggested that the structure and performance of broken and re-grown flocs were dependent on the effective coagulation time under the same hydraulic conditions. However, we can only receive approximate information regarding the characterization evolution of flocs from these feasible tests. To investigate the detailed breakage procedure of flocs in-depth, we must apply numerical methods to discuss this phenomenon.

Effect of re-growing time on evolution of floc structure

To further study the possible growth mechanisms of broken flocs in the re-growth process, flocculation tests were carried out just as before. First, slow stirring was done for 20 min until the values of average radius and fractal dimension reached a stable stage, and stirring at 300 rpm/min was then done for 1 min until breakage. Finally, for the re-forming time, different values from 5 to 20 min were adopted. The mixing duration and shear force of the aggregation and breakage stages were set as coincident during the flocculation tests, and the morphological characteristic values of flocs were fitted at each time for comparison. The dynamic evolution curves of average radius and fractal dimension for various re-growing times are shown in Fig. 7.

The values of average radius and D_{pf} promptly increased for the re-growing times of 5 and 10 min, which suggests that there was an obvious reversibility in the early stage of the re-growth procedure and the relatively compact broken flocs rapidly grew to slightly larger and looser ones. It is likely that the gentle hydraulic condition enhanced the sticking probability between free particles and existing clusters. For 15 min of re-growth, the values of average radius and D_{pf} increased as the time increased until the limited values of floc size and fractal structure were reached and then declined as time increased. However, for 20 min of re-growth, both the average radius and the fractal dimension reached lower plateaus. It can be seen that a longer reaction time could promote the relative motion between different-sized particles and probably provide more opportunities for suspended particles to adhere to larger clusters. However, coagulant aging could weaken the sticking capacity among particles, which most likely reduced the compactness of re-grown flocs during longer re-growth time. Thus, the re-grown flocs had great possibilities to break again and further aggravate the deterioration of floc structure. However, all of the conclusions were also speculations based on the experimental data, which makes it difficult to retrieve the specific changing process of floc morphology during the re-growth period.

Compared with the evolution of floc morphology during the whole flocculation process, the reaction time mainly influenced the formation of flocs. However, the changing mechanism and evolution procedure of floc structure and features

under different reaction times were clear because they could not be determined by using the limited experimental methods. Thus, the modified two-dimensional DLA model and a simplified floc breakage approach were utilized in this study. Using these numerical methods, we attempted to study the visualization of floc characteristics over different reaction times.

Morphological characteristics using two-dimensional DLA model

As discussed above, the reaction time has a strong influence on the morphological characteristics of flocs in practical experiments. A two-dimensional DLA model was investigated to study the evolution of floc morphology throughout the flocculation process. To weaken random effects, the same simulation was conducted multiple times and the characteristic indexes were calculated for each instance. The results shown in Fig. 8 reveal that every index tended to become stable after ten simulations. Thus, virtual flocs were simulated under every condition ten times, and the average values of the determined indexes were taken.

Effect of msa on virtual floc

The eventual configurations of simulated flocs from the improved two-dimensional DLA model with different values of msa are shown in the first row of Fig. 9. The D_{pf} and porosity ratios of virtual flocs are included as footnotes at the left bottom of every sub-image. For the least aggregated steps ($msa=200$), no obvious fractal feature of the virtual floc was observed. At a slightly longer aggregated duration ($msa=500$), the virtual floc gradually grew toward the preponderant direction and irregular branches emerged. However, for $msa=1000$, the branches of the virtual floc grew more and more in every direction. Floc size increased with the extension of aggregation time during the aggregation process, which was similar to the results obtained using the experimental method. Based on the DLA numerical simulation, it was clear that particles usually grew toward the strong branches without the occurrence of breakage during the procedure. The long and robust branches had more opportunities to catch the suspended particles, which inhibited the growth of shorter branches. This shielding effect also made it difficult for free particles to enter the inner part of the virtual flocs.

Moreover, although flocs with less msa seemed to be compact, the values of D_{pf} were smaller. This result most likely implied that floc structure was not yet fully developed, which was expected because this type of floc should have a rather poor solid-liquid separation capacity. However, for longer msa , free particles easily adhered to the developed branches of virtual flocs and urged the flocs to gradually grow more branches and become rough. In the practical test, floc size did

not increase over too long aggregation time, which may have been due to breakage originating from the weaker strength of flocs. The results indicate that the value of msa could intensively reflect the effects of aggregation time on the growing process of flocs in the simulation and that reasonable control of the msa is important to produce flocs with the desired structures and properties.

Effect of breakage method

Based on the simplified method of breakage presented in [Simple breakage model](#) section, the configurations of broken flocs are shown in the second row of Fig. 9. The visualization illustrates that there were obvious distinctions regarding the structure and granularity of flocs before and after breakage, which was independent of the msa values. The differences between the maximum and minimum characteristic lengths before breakage (the values of $a1$, $b1$, and $c1$ in Table 1) were, respectively, 12.16, 11.37, and 17.6, which correspond to the msa values; these differences between broken flocs (values of $a2$, $b2$, and $c2$ in Table 1) always tended to be approximate.

The results better indicated that there was a critical moment when floc structure transferred from isotropic to anisotropic and the growth inhibition of branches was strengthened. Moreover, the flocs that formed before breakage had many more irregular branches, especially in the areas away from the seed, for the reasons noted above. Nevertheless, the ruleless branches of broken flocs began to decrease, and there were considerable drops in both the porosity ratio and fractal dimension of broken flocs after breakage. Similarly, the average sizes of flocs dramatically declined when the shear force significantly increased in the tests.

These results were shown in the simulation, which suggested that the particles' occupancy within the gyration radius increased and that the grain density of virtual flocs improved due to breakage. For msa of 500 and 1000, the differences of D_{pf} between before and after the breakage of flocs were 0.07 and 0.03, respectively. However, there was an appreciable reduction of the porosity ratio of broken flocs under the same conditions. We speculated that the breakage process only removed the particles away from the seed; hence, the significant decline of porosity ratio did not cause a great change in the flocs' fractal structures. The particle size distribution near the seed played a decisive role in the virtual floc compactness, whereas particles away from the seed hardly contributed to the compactness of virtual flocs. Wu et al. (2013) stated that fractal dimension decreases significantly as the radius of the primary particle increases and that the initial particles play an important role in the shape of flocs. The difference between the D_{pf} of flocs before and after breakage became increasingly inconspicuous as the msa increased, which may have been due to the much stronger self-similarity of flocs, which, in turn, had little impact on the fractal characteristics of broken flocs.

Effect of *msr* on virtual floc

Some researchers have proven that broken flocs will recover under suitable hydraulic conditions via experimental means (Barbot et al. 2010; Zhao et al. 2013). In the flocculation tests, we also found that different re-growing time caused various results in our research. However, the testing methods could not observe the microscopic changes of floc structure during the flocculation process. To visualize the re-structuring of broken flocs under various *msr* values, a modified simulation was conducted; specific operations were described in **Materials and methods** section. Considering the broken flocs to be aggregated cores, the re-growth process occurred between small clusters and scattered particles in this mimic flocculation system. The final shapes of re-aggregated virtual flocs under various values of *msr* are exhibited in Fig. 10. The gray particles represent the aggregated core, and the re-grown particles are shown in red. The porosity ratio and D_{pf} of every floc are also labeled at the left bottom of every sub-image, as in Fig. 9.

The re-grown virtual flocs at an *msr* of 200 under different aggregated cores are shown in the first row of Fig. 10. The released free particles mainly adhered to the boundary of the aggregated core, which was closely packed with a few branches. The values of porosity ratio and D_{pf} of these re-grown flocs were similar to those corresponding to broken flocs but were smaller than those of flocs before breakage. Then, with an *msr* value of 1000 (corresponding to a4, b4, and c4 in Fig. 10), the characteristic lengths (values of a4, b4, and c4 in Table 1) of the re-grown virtual flocs were slightly greater than those before breakage and distinct branches developed around the aggregated cores. The characteristic lengths of re-grown virtual flocs become rather uniform compared to those of flocs before breakage. This result could illustrate that free particles have similar chances to be captured by the branches and that the mutual inhibition among the branches was relatively weaker. In this case, the branched structure of flocs was improved during the restructuring process. Furthermore, the structure of broken flocs impacted the features of re-grown flocs. Comparing the characteristic lengths of virtual re-grown flocs with the same *msr* (values of a3, b3, c3 and a4, b4, c4 in Table 1), more branched flocs existed for larger values of *msa*. It seems that the broken flocs formed with smaller *msa* values had fewer potential connection points for re-growth than did those formed with larger values.

The results of the investigation of changes in the characteristic indexes of re-grown flocs indicate that the flocs could recover their original size after breakage and re-growth and become even larger than they were before breakage. When they were formed at smaller values of *msr*, the broken flocs had few opportunities to gather with other particles, thus causing limited reconnection. However, it seems that re-grown virtual flocs have fairly more branches at greater *msr* values.

This may occur because a longer reaction time of the re-growth process indirectly improves the chances of cores to capture free particles, thereby promoting the development of new branches. However, the existence of the shielding effect could hinder shorter branches from further growth. As a result, the number of particles in the interior of the gyration radius was reduced.

However, the values of the porosity ratio and D_{pf} of re-grown flocs were both lower than those of the original flocs, which indicated that the properties of flocs were improved after the breakage and re-growth processes. Additionally, comparing the characteristic features of re-grown flocs produced under different *msr* values, relatively integrated and mature flocs formed at larger *msr* values. Thus, a slightly longer re-growing time resulted in enhanced floc morphological characteristics. However, if the re-growing time was too long, it is speculated that rough and fragile flocs with poor stability would develop.

Conclusion

The dynamic variation of floc structure for different hydraulic retention times in the flocculation process has been investigated via experimental analysis and numerical simulation. Through a combination of testing and simulated results, this study presents an in-depth discussion of the behavior of floc breakage and the fractal growth of flocs.

1. Under the same conditions, different configurations of flocs formed after breakage under various HRT, thus significantly affecting floc structure during the re-forming process. In flocculation tests, a shorter aggregation time produced smaller flocs. After breakup, more growing sites were exposed to give more chances for scattered particles to adhere in the following process. For the early stage of re-growth, broken pieces rapidly aggregated to slightly larger ones, whereas open and porous flocs gradually formed as the reaction time increased. The broken flocs formed for a shorter aggregation time had the capacity for complete recovery, but for a longer reaction time, a rather worse reversibility of the broken flocs existed.
2. The maximum motion step of a particle was added to the classic two-dimensional DLA model to introduce the time concept in the static model and to further discuss the impact of time on the changes of floc characterization. Both the size and compactness of flocs improved as the maximum motion step increased, independent of the aggregation and re-formation processes. However, many more steps could weaken the compactness of flocs and very likely induce breakage. A transition for flocs from isotropic to anisotropic as *msa* increased was found, and the compactness of flocs was mainly affected by the

distribution of particles near the aggregated core instead of those far away.

3. A simplified breakage model of flocs, based on the two typical strength models of Rumpf and Kendall, was proposed to study the visualization of the breakage/re-formation process. The peripheral branches of virtual flocs were destroyed by breakage, and the vacant adhesion sites were exposed, which produced isotropic floc pieces. Broken flocs provided more chances for free particles to enter into the inner parts of flocs and to become uniformly packed around the aggregated core, thus becoming re-available to improve the structure and properties of flocs in the subsequent re-growing process. Because broken flocs composed the re-aggregated core, visualization results show that the floc fragments formed for larger m_{sa} values had more growing sites than did those of smaller m_{sa} values, which benefitted the reforming procedure.

Acknowledgments This research was supported by the National Science and Technology Major Project of Twelfth Five Years (Grant No. 2014ZX07201-012-2, Grant No. 2013ZX07201007-002), the National Innovation Team supported by the National Science Foundation of China (Grant No. 50821002), and the State Key Laboratory of Urban Water Resource and Environment (Harbin Institute of Technology) (Grant No. 2012DX07). Comments and suggestions from anonymous reviewers are greatly acknowledged.

Reference

- Amitrano C, Coniglio A, Meakin P, Zannetti M (1991) Multiscaling in diffusion-limited aggregation. *Phys Rev B* 44:4974–4977
- Barbot E, Dussouillez P, Bottero JY, Moulin P (2010) Coagulation of bentonite suspension by polyelectrolytes or ferric chloride: floc breakage and reformation. *Chem Eng J* 156:83–91
- Biggs CA, Lant PA (2000) Activated sludge flocculation: on-line determination of floc size and the effect of shear. *Water Res* 34:2542–2550
- Chakraborti RK, Atkinson JF, Van Benschoten JE (2000) Characterization of alum floc by image analysis. *Environ Sci Technol* 34:3969–3976
- Duan J, Gregory J (1998) The influence of silicic acid on aluminium hydroxide precipitation and flocculation by aluminium salts. *J Inorg Biochem* 69:193–201
- Rumpf H (1962) Agglomeration. Wiley Intersci 379–418
- He W, Nan J, Li H, Li S (2012) Characteristic analysis on temporal evolution of floc size and structure in low-shear flow. *Water Res* 46:509–20
- Higashitani K, Imura K, Sanda H (2001) Simulation of deformation and breakup of large aggregates in flows of viscous fluids. *Chem Eng Sci* 56:2927–2938
- Hopkins DC, Ducoste JJ (2003) Characterizing flocculation under heterogeneous turbulence. *J Colloid Interface Sci* 264:184–194
- Jarvis P, Jefferson B, Gregory J, Parsons SA (2005) A review of floc strength and breakage. *Water Res* 39:3121–3137
- Kendall K, Alford NM, Tan SR, Birchall JD (1986) Influence of toughness on Weibull modulus of ceramic bending strength. *J Mater Res* 1:120–123
- McCurdy K, Carlson K, Gregory D (2004) Floc morphology and cyclic shearing recovery: comparison of alum and polyaluminum chloride coagulants. *Water Res* 38:486–494
- McFarlane A, Bremmell K, Addai-Mensah J (2006) Improved dewatering behavior of clay minerals dispersions via interfacial chemistry and particle interactions optimization. *J Colloid Interface Sci* 293:116–127
- Meakin P, Vicsek T (1987) Diffusion-limited aggregation with radial bias. *J Phys A Math Gen* 20:L171
- Meakin P, Skjeltorp AT (1993) Application of experimental and numerical models to the physics of multiparticle systems. *Adv Phys* 42:1–127
- Mikkelsen LH, Keiding K (2002) Physico-chemical characteristics of full scale sewage sludges with implications to dewatering. *Water Res* 36:2451–2462
- Mpofu P, Addai-Mensah J, Ralston J (2003) Investigation of the effect of polymer structure type on flocculation, rheology and dewatering behaviour of kaolinite dispersions. *Int J Miner Process* 71:247–268
- Mpofu P, Addai-Mensah J, Ralston J (2004) Flocculation and dewatering behaviour of smectite dispersions: effect of polymer structure type. *Miner Eng* 17:411–423
- Nan J, He W, Song X, Li G (2009) Impact of dynamic distribution of floc particles on flocculation effect. *J Environ Sci* 21:1059–1065
- Nan J, He W (2012) Characteristic analysis on morphological evolution of suspended particles in water during dynamic flocculation process. *Desalin Water Treat* 41:35–44
- Parkinson J, Brechet Y, Gordon R (1999) Centric diatom morphogenesis: a model based on a DLA algorithm investigating the potential role of microtubules. *Biochim Biophys Acta* 1452:89–102
- Serra T, Colomer J, Casamitjana X (1997) Aggregation and breakup of particles in a shear flow. *J Colloid Interface Sci* 187:466–473
- Sun CZ, Yue QY, Gao BY, Mu RM, Liu J, Zhao YX, Yang ZL, Xu WY (2011) Effect of pH and shear force on flocs characteristics for humic acid removal using polyferric aluminum chloride-organic polymer dual-coagulants. *Desalination* 281:243–247
- Turchiuli C, Fargues C (2004) Influence of structural properties of alum and ferric flocs on sludge dewaterability. *Chem Eng J* 103:123–131
- Wahlberg EJ, Keinath TM, Parker DS (1994) Influence of activated sludge flocculation time on secondary clarification. *Water Environ Res* 66:779–786
- Wang D, Wu R, Jiang Y, Chow CWK (2011) Characterization of floc structure and strength: role of changing shear rates under various coagulation mechanisms. *Colloids Surf A* 379:36–42
- Wei J, Gao B, Yue Q, Wang Y, Li W, Zhu X (2009) Comparison of coagulation behavior and floc structure characteristic of different polyferric-cationic polymer dual-coagulants in humic acid solution. *Water Res* 43:724–732
- Wenzheng Y (2010) Breakage and regrowth of Al-humic floc-effect of additional coagulant dosage. *Environ Sci Technol* 44:6
- Witten TA, Sander LM (1981) Diffusion-limited aggregation, a kinetic critical phenomenon. *Phys Rev Lett* 47:1400–1403
- Wu H, Lattuada M, Morbidelli M (2013) Dependence of fractal dimension of DLCA clusters on size of primary particles. *Adv Colloid Interf* 195–196:41–49
- Xiao F, Lam KM, Li XY, Zhong RS, Zhang XH (2011) PIV characterization of flocculation dynamics and floc structure in water treatment. *Colloids Surf A* 379:27–35
- Xu W, Gao B, Yue Q, Wang Y (2010) Effect of shear force and solution pH on flocs breakage and re-growth formed by nano-Al13 polymer. *Water Res* 44:1893–1899
- Yao M, Nan J, Chen T (2014) Effect of particle size distribution on turbidity under various water quality levels during flocculation processes. *Desalination* 354:116–124
- Yao M, Nan J, Chen T, Zhan D, Li Q, Wang Z, Li H (2015) Influence of flocs breakage process on membrane fouling in coagulation/ultrafiltration process—effect of additional coagulant of poly aluminium chloride and polyacrylamide. *J Membr Sci*
- Yao M, Nan J, Li Q, Zhan D, Chen T, Wang Z, Li H (2016) Effect of under-dosing coagulant on coagulation-ultrafiltration process for

- treatment of humic-rich water with divalent calcium ion. *J Membr Sci*, JMS151005
- Yeung AKC, Pelton R (1996) Micromechanics: a new approach to studying the strength and breakup of flocs. *J Colloid Interface Sci* 184:579–585
- Yu W, Hu C, Liu H, Qu J (2012) Effect of dosage strategy on Al-humic flocs growth and re-growth. *Colloids Surf A* 404:106–111
- Yukselen MA, Gregory J (2004) The reversibility of floc breakage. *Int J Miner Process* 73:251–259
- Zhao YX, Gao BY, Shon HK, Wang Y, Kim JH, Yue QY (2011) The effect of second coagulant dose on the regrowth of flocs formed by charge neutralization and sweep coagulation using titanium tetrachloride (TiCl₄). *J Hazard Mater* 198:70–77
- Zhao YX, Gao BY, Qi QB, Wang Y, Phuntsho S, Kim JH, Yue QY, Li Q, Shon HK (2013) Cationic polyacrylamide as coagulant aid with titanium tetrachloride for low molecule organic matter removal. *J Hazard Mater* 258:84–92
- Zhong R, Zhang X, Xiao F, Li X (2011) Effects of humic acid on recoverability and fractal structure of alum-kaolin flocs. *J Environ Sci* 23: 731–737